RF and Microwave Transistor Oscillator Design

RF and Microwave Transistor Oscillator Design

Andrei Grebennikov
Infineon Technologies AG, Germany

BICENTENNIAL 1807 WILEY 2007
John Wiley & Sons, Ltd

Telephone (+44) 1243 779777

Email (for orders and customer service enquiries): cs-books@wiley.co.uk
Visit our Home Page on www.wiley.com

Other Wiley Editorial Offices

John Wiley & Sons Inc., 111 River Street, Hoboken, NJ 07030, USA

Jossey-Bass, 989 Market Street, San Francisco, CA 94103-1741, USA

Wiley-VCH Verlag GmbH, Boschstr. 12, D-69469 Weinheim, Germany

John Wiley & Sons Australia Ltd, 42 McDougall Street, Milton, Queensland 4064, Australia

John Wiley & Sons (Asia) Pte Ltd, 2 Clementi Loop #02-01, Jin Xing Distripark, Singapore 129809

John Wiley & Sons Canada Ltd, 6045 Freemont Blvd, Mississauga, ONT, Canada L5R 4J3

Wiley also publishes its books in a variety of electronic formats. Some content that appears in print may not be available in electronic books.

Anniversary Logo Design: Richard J. Pacifico

British Library Cataloguing in Publication Data

A catalogue record for this book is available from the British Library

ISBN 978-0-470-02535-2 (HB)

Typeset in 10/12pt Times Roman by TechBooks, New Delhi, India.
Printed and bound in Great Britain by Antony Rowe Ltd, Chippenham, Wiltshire
This book is printed on acid-free paper responsibly manufactured from sustainable forestry in which at least two trees are planted for each one used for paper production.

Contents

About the Author **ix**

Preface **xi**

Acknowledgements **xv**

1 Nonlinear circuit design methods **1**
1.1 Spectral-domain analysis 1
1.1.1 Trigonometric identities 2
1.1.2 Piecewise-linear approximation 4
1.1.3 Bessel functions 8
1.2 Time-domain analysis 9
1.3 Newton–Raphson algorithm 12
1.4 Quasilinear method 15
1.5 Van der Pol method 20
1.6 Computer-aided analysis and design 24
References 28

2 Oscillator operation and design principles **29**
2.1 Steady-state operation mode 29
2.2 Start-up conditions 31
2.3 Oscillator configurations and historical aspects 36
2.4 Self-bias condition 43
2.5 Oscillator analysis using matrix techniques 50
2.5.1 Parallel feedback oscillator 50
2.5.2 Series feedback oscillator 53
2.6 Dual transistor oscillators 55
2.7 Transmission-line oscillator 60
2.8 Push–push oscillator 65
2.9 Triple-push oscillator 72
2.10 Oscillator with delay line 75
References 79

3 Stability of self-oscillations **83**
3.1 Negative-resistance oscillator circuits 83
3.2 General single-frequency stability condition 86
3.3 Single-resonant circuit oscillators 87
3.3.1 Series resonant circuit oscillator with constant load 87
3.3.2 Parallel resonant circuit oscillator with nonlinear load 88
3.4 Double-resonant circuit oscillator 89
3.5 Stability of multi-resonant circuits 91
3.5.1 General multi-frequency stability criterion 91
3.5.2 Two-frequency oscillation mode and its stability 93
3.5.3 Single-frequency stability of oscillator with two coupled resonant circuits 94
3.5.4 Transistor oscillators with two coupled resonant circuits 96
3.6 Phase plane method 105
3.6.1 Free-running oscillations in lossless resonant LC circuits 106
3.6.2 Oscillations in lossy resonant LC circuits 108
3.6.3 Aperiodic process in lossy resonant LC circuits 110
3.6.4 Transformer-coupled MOSFET oscillator 112
3.7 Nyquist stability criterion 113
3.8 Start-up and stability 118
References 125

4 Optimum design and circuit technique **127**
4.1 Empirical optimum design approach 128
4.2 Analytic optimum design approach 136
4.3 Parallel feedback oscillators 138
4.3.1 Optimum oscillation condition 138
4.3.2 Optimum MOSFET oscillator 139
4.4 Series feedback bipolar oscillators 142
4.4.1 Optimum oscillation condition 142
4.4.2 Optimum common base oscillator 143
4.4.3 Quasilinear approach 146
4.4.4 Computer-aided design 150
4.5 Series feedback MESFET oscillators 152
4.5.1 Optimum common gate oscillator 152
4.5.2 Quasilinear approach 154
4.5.3 Computer-aided design 157
4.6 High-efficiency design technique 162
4.6.1 Class C operation mode 162
4.6.2 Class E power oscillators 165
4.6.3 Class DE power oscillators 170
4.6.4 Class F mode and harmonic tuning 172
4.7 Practical oscillator schematics 177
References 182

5 Noise in oscillators **187**
5.1 Noise figure 187
5.2 Flicker noise 196
5.3 Active device noise modelling 198
5.3.1 MOSFET devices 198
5.3.2 MESFET devices 200
5.3.3 Bipolar transistors 203
5.4 Oscillator noise spectrum: linear model 205
5.4.1 Parallel feedback oscillator 205
5.4.2 Negative resistance oscillator 214
5.4.3 Colpitts oscillator 216
5.5 Oscillator noise spectrum: nonlinear model 219
5.5.1 Kurokawa approach 219
5.5.2 Impulse response model 224
5.6 Loaded quality factor 235
5.7 Amplitude-to-phase conversion 239
5.8 Oscillator pulling figure 241
References 245

6 Varactor and oscillator frequency tuning **251**
6.1 Varactor modelling 251
6.2 Varactor nonlinearity 255
6.3 Frequency modulation 258
6.4 Anti-series varactor pair 262
6.5 Tuning linearity 267
6.5.1 VCOs with lumped elements 267
6.5.2 VCOs with transmission lines 273
6.6 Reactance compensation technique 276
6.7 Practical VCO schematics 280
6.7.1 VCO implementation techniques 280
6.7.2 Differential VCOs 286
6.7.3 Push–push VCOs 292
References 296

7 CMOS voltage-controlled oscillators **299**
7.1 MOS varactor 299
7.2 Phase noise 305
7.3 Flicker noise 310
7.4 Tank inductor 313
7.5 Circuit design concepts and technique 317
7.5.1 Device operation modes 317
7.5.2 Start-up and steady-state conditions 321
7.5.3 Differential cross-coupled oscillators 325
7.5.4 Wideband tuning techniques 326
7.5.5 Quadrature VCOs 331

7.6 Implementation technology issues 333
7.7 Practical schematics of CMOS VCOs 335
References 342

8 Wideband voltage-controlled oscillators 347
8.1 Main requirements 347
8.2 Single-resonant circuits with lumped elements 351
8.2.1 Series resonant circuit 351
8.2.2 Parallel resonant circuit 353
8.3 Double-resonant circuit with lumped elements 356
8.4 Transmission line circuit realization 360
8.4.1 Oscillation system with uniform transmission line 360
8.4.2 Oscillation system with multi-section transmission line 365
8.5 VCO circuit design aspects 369
8.5.1 Common gate MOSFET and MESFET VCOs 369
8.5.2 Common collector bipolar VCO 373
8.5.3 Common base bipolar VCO 376
8.6 Wideband nonlinear design 378
8.7 Dual mode varactor tuning 381
8.8 Practical RF and microwave wideband VCOs 387
8.8.1 Wireless and satellite TV applications 387
8.8.2 Microwave monolithic VCO design 391
8.8.3 Push–push oscillators and oscipliers 394
References 396

9 Noise reduction techniques 399
9.1 Resonant circuit design technique 399
9.1.1 Oscillation systems with lumped elements 400
9.1.2 Oscillation systems with transmission lines 402
9.2 Low-frequency loading and feedback optimization 410
9.3 Filtering technique 416
9.4 Noise-shifting technique 423
9.5 Impedance noise matching 426
9.6 Nonlinear feedback loop noise suppression 430
References 433

Index 437

About the Author

Dr Andrei Grebennikov, IEEE Senior Member, has obtained long-term academic and industrial experience. He worked with Moscow Technical University of Telecommunications and Informatics, Russia; Institute of Microelectronics, Singapore; M/A-COM, Ireland and Infineon Technologies, Germany, as an engineer, researcher, lecturer and educator.

Dr Grebennikov has lectured as a Guest Professor in University of Linz, Austria, and presented short courses as an Invited Speaker at the International Microwave Symposium, European Microwave Conference and Motorola Design Centre, Malaysia. He is also the author of more than 60 papers, 3 books and several US patents.

Preface

The main objective of this book is to present all relevant information necessary for RF and microwave transistor oscillator design including well-known and new theoretical approaches and practical circuit schematics and designs, as well as to suggest optimum design approaches, which combine effectively analytic calculations and computer-aided design. This book can be useful for lecturing to promote the analytical way of thinking and combine effectively theory and practice of RF and microwave engineering. As often happens, a new result is a long-forgotten old one. Therefore, not only new results based on new technologies or circuit schematics are given, but some old ideas, schematics or approaches are also introduced, that could be very useful in modern practice or could contribute to the development of new ideas or techniques.

As a result, this book is intended for and can be recommended to:

- *university-level professors and researchers*, as possible reference and well-founded material for creative research and teaching activity which will contribute to strong background for graduates and postgraduates students;
- *R&D staff*, to combine the theoretical analysis and practical aspects, including computer-aided design (CAD) and to provide a sufficient basis for new ideas in theory and practical circuit techniques;
- *practising RF designers and engineers*, as an anthology of many well-known and new practical transistor oscillator circuits with detailed descriptions of their operational principles and applications and clear practical demonstration of theoretical results.

Chapter 1 presents the most commonly used design techniques for analysing nonlinear circuits, in particular, transistor oscillators. There are several approaches to analyse and design nonlinear circuits, depending on their main specifications. That means an analysis both in the time domain to determine transient circuit behaviour and in the frequency domain to improve power and spectral performances when parasitic effects such as instability and spurious emission must be eliminated or minimized. Using the time-domain technique, it is relatively easy to describe a nonlinear circuit with differential equations, which can be solved analytically in explicit form for only some simple cases. Under the assumption of slowly varying amplitude and phase, it is possible to obtain the separate truncated first-order differential equations for the amplitude and phase of the oscillation process from the original second-order nonlinear differential equation. However, generally it is necessary to use numerical methods. The time-domain analysis is limited to its inability to operate with the circuit immittance (impedance or admittance) parameters as well as the fact that it can be practically applied only for circuits with lumped parameters or ideal transmission lines. The frequency-domain analysis is less ambiguous because a relatively complex circuit can often be reduced to one or more sets of immittances at each harmonic component. For example, using a quasilinear approach, the nonlinear circuit parameters averaged by the fundamental component allow one to apply a linear circuit analysis. Advanced modern CAD simulators incorporate both time-domain and frequency-domain methods as well as optimization techniques to provide all the necessary design cycles.

Chapter 2 introduces the principles of oscillator design, including start-up and steady-state operation conditions, basic oscillator configurations using lumped and transmission-line elements and simplified equation-based oscillator analysis and design techniques. An immittance design approach is introduced and applied to series and parallel feedback oscillators, including circuit design and simulation aspects. Numerous practical examples of RF and microwave oscillators using MOSFET, MESFET and bipolar devices, including the descriptions of their circuit realizations, are given.

Applying dc bias to the active device does not generally result in the negative resistance condition. This condition has to be induced in these devices and it is determined by the physical mechanism in the device and chosen circuit topology. The transistor in the oscillator circuits is mostly represented as the active two-port network, whose operation principle is reflected through its equivalent circuit. The influence of the circuit and transistor parameters can result in a hysteresis effect or oscillation instability in practical design. In high-frequency practical implementation, the presence of the parasitic device and circuit elements can contribute to the multi-resonant circuits. The possibility of an operation mode with different natural frequencies depends on the value of the coupling coefficient between resonant circuits. Therefore, the stability conditions for a steady-state single-frequency operation for a multi-resonant circuit, in general, and two coupled resonant circuits, in particular, are analytically derived. The several examples of stability criteria for different single-resonant and double-resonant oscillator circuits are described and analysed in Chapter 3. In addition, the phase plane method as a qualitative method of an analysis of the dynamics of the oscillation systems and a Nyquist stability criterion are shown and illustrated by several examples of the oscillator circuits described by second-order differential equations.

Generally, RF and microwave transistor oscillator design is a complex problem. Depending on the technical requirements, it is necessary to define the configuration of the oscillator circuit, choose a proper transistor type, evaluate and measure the parameters of the transistor nonlinear model under small- and large-signal conditions. Finally, an appropriate nonlinear simulator must be used to simulate the oscillator performance in time and frequency domains. An oscillator analysis can be based on the two-port network approach to describe the active device and feedback circuit. In this case, the basic parameters of the transistor equivalent circuit can be directly measured, or approximated on the basis of experimental data, with sufficient accuracy across a wide frequency range. However, the values of the external feedback circuit elements are initially unknown. The process of determining the optimum values of the feedback and load parameters can be time-consuming and, in a typical case, calls for much simulation. Consequently, it is convenient to use an analytic method of optimizing oscillator design. This method should incorporate the explicit expressions for feedback elements and load impedance in terms of the transistor equivalent circuit elements and its static volt–ampere and voltage–capacitance characteristics. Chapter 4 presents both the empirical and analytic optimum design approaches applied to series and parallel feedback oscillators, including circuit design and simulation aspects, and high-efficiency design techniques as well. Typical practical examples of RF and microwave oscillators using MOSFET, MESFET, HEMT, and bipolar devices, including the descriptions of their circuit configurations, are given.

Chapter 5 describes different oscillator noise models to express a clear relationship between the resonant circuit and active device noise model parameters. The simple Leeson linear model for a feedback oscillator, which was derived empirically, is based on the expectations that the contribution to the real oscillator output spectrum is provided by two basic processes. The first process is a result of the phase fluctuations due to the additive white noise at frequency offsets close to the carrier. The second process is a result of the low-frequency fluctuations or flicker noise up-converted to the carrier region because of the active device nonlinear effects. The nonlinear Kurokawa analysis based on the sinusoidal representation of the current in the negative-resistance oscillator extends the oscillator noise model by introducing relationships between the noise power, stability conditions and amplitude-to-phase conversion. However, such a noise generation mechanism does not consider the mixing effect from the inherent nonlinear behaviour of the active device when the current at the output of the active device must be represented by a Fourier series expansion. Thus, the phase noise generated around the fundamental frequency of the oscillation generally is an equal contribution of two simultaneous and correlated phenomena: additive phase noise due to phase modulation process and converted phase noise due to conversion from one sideband to another.

Voltage-controlled oscillators are key components in many applications, especially in wireless communication systems, measurement equipment, or military applications. A growing market of wireless applications requires highly integrated circuit solutions, where both high-performance transistors and passive elements with high quality factors can be used. Chapter 6 discusses the varactor modelling issues, varactor nonlinearity and its effect to frequency modulation, and resonant circuit techniques to improve VCO tuning linearity using lumped and transmission-line elements. Various practical examples of VCO implementation techniques based on using different types of active devices, circuit schematic approaches and hybrid or monolithic integrated circuit technologies are shown and described.

The rapid growth of new-generation wireless communication systems has created a strong demand for designing single-chip radio transceivers in a fully monolithic CMOS process with extremely small size due to better integration, low cost and low operating voltage. To increase the integration level, all passive components must be integrated monolithically into a single chip. In this case, the elements of a resonant *LC* circuit of the voltage-controlled oscillator as a core part of the synthesizers should feature high quality factors over frequency tuning range. Chapter 7 discusses the technological aspects to realize MOS varactors and spiral inductors, basic concepts of circuit design and implementation issues, oscillator phase noise and the effect of low-frequency flicker noise. Also included are various practical examples of differential, complementary and quadrature CMOS VCOs using different process technologies.

Wideband voltage-controlled oscillators are used in a variety of RF and microwave systems, including broadband measurement equipment, wireless and TV applications and military electronic countermeasure systems. Among wideband tunable signal sources such as YIG-tuned oscillators, wideband VCOs are preferable because of their small size, low weight, high settling time speed and capability of fully monolithic integration. Therefore, modern radar and communication applications demand VCOs that are capable of being swept across a wide range of potential threat frequencies with a speed and settling time far beyond that of the YIG-tuned oscillators. This chapter discusses the basic concepts of wideband VCO circuit design and gives specific circuit solutions using lumped elements and transmission lines to improve their frequency tuning characteristics. Various examples of the RF and microwave VCO circuit configurations using bipolar, MOSFET and MESFET devices are analysed, their circuit parameters are calculated or optimized to provide maximum tuning bandwidth or minimum tuning linearity. Also included are numerous practical examples of wideband VCOs for RF and microwave applications in radar or telecommunication systems.

Chapter 9 discusses phase noise reduction techniques and gives specific resonant circuit solutions using lumped and distributed parameters for frequency stabilization and phase noise reduction. Phase noise improvement can also be achieved by appropriate low-frequency loading and feedback circuitry optimization. The feedback system incorporated into the oscillator bias circuit can provide significant phase noise reduction over a wide frequency range from the high frequencies up to microwaves. Particular discrete implementations of a bipolar oscillator with collector and emitter noise feedback circuits are described. Also a filtering technique based on a passive *LC* filter to lower the phase noise in the differential oscillator is presented. Several topologies of fully integrated CMOS voltage-controlled oscillators using filtering techniques are shown and discussed. A novel noise-shifting differential VCO based on a single-ended classical three-point circuit configuration with common base can improve the phase noise performance by a proper circuit realization. An optimal design technique using an active element based on a tandem connection of a common source FET device and a common base bipolar transistor with optimum coupling of the active element to the resonant circuit is presented. The phase noise in microwave oscillators can also be reduced using negative resistance compensation increasing the loaded quality factor of the oscillator resonant circuit. Finally, a new approach utilizing a nonlinear feedback loop for phase noise suppression in microwave oscillators is discussed.

Acknowledgements

Dr Vladimir Nikiforov who was a patient tutor and wise teacher during our long-term joint research work at the Moscow Technical University of Communications and Informatics and whose invaluable human and scientific features have contributed to the author's research and publishing creative activity.

Dr Bill Chen, the first Director of the Institute of Microelectronics, Singapore, for making it possible to use the institute's excellent facilities and environment without which this book project could not be realized.

Alex Teo and his colleagues from Ansoft Corporation for their excellent professional software products and valuable technical assistance.

Ravinder Walia for helpful and useful discussions of CMOS oscillator design issues.

Prof Grigory Aristarkhov, Dr Vladimir Chernyshev, Dr Pavel Mikhnevich, Dr Vladimir Pashnin, Dr Nikolai Paushkin and Dr Elena Stroganova from the Moscow Technical University of Communications and Informatics, Russia; Dr Herbert Jaeger from the University of Linz, Austria; Dr Alberto Costantini from the University of Bologna, Italy; and Dr Rajinder Singh and Dr Lin Fujiang from the Institute of Microelectronics, Singapore, for encouragement and support.

The author especially wishes to thank his wife, Galina Grebennikova, for performing important numerical calculations and computer artwork design, as well as for her constant encouragement, inspiration, support and assistance.

Finally, I would like to express my sincere appreciation to all the staff at John Wiley & Sons involved in this publishing project for their cheerful professionalism and outstanding efforts.

1

Nonlinear circuit design methods

This chapter presents the most commonly used design techniques for analysing nonlinear circuits, in particular, transistor oscillators. There are several approaches to analyse and design nonlinear circuits, depending on their main specifications. This means an analysis both in the time domain to determine transient circuit behaviour and in the frequency domain to improve power and spectral performances when parasitic effects such as instability and spurious emission must be eliminated or minimized. Using the time-domain technique, it is relatively easy to describe a nonlinear circuit with differential equations, which can be solved analytically in explicit form for only a few simple cases. Under an assumption of slowly varying amplitude and phase, it is possible to obtain separate truncated first-order differential equations for the amplitude and phase of the oscillation process from the original second-order nonlinear differential equation. However, generally it is required to use numerical methods. The time-domain analysis is limited to its inability to operate with the circuit immittance (impedance or admittance) parameters as well as the fact that it can be practically applied only for circuits with lumped parameters or ideal transmission lines. The frequency-domain analysis is less ambiguous because a relatively complex circuit can often be reduced to one or more sets of immittances at each harmonic component. For example, using a quasilinear approach, the nonlinear circuit parameters averaged by fundamental component allow one to apply a linear circuit analysis. Advanced modern CAD simulators incorporate both time-domain and frequency-domain methods as well as optimization techniques to provide all necessary design cycles.

This chapter also includes a brief introduction of simulator tools based on the Ansoft Serenade circuit simulator. In addition, some practical equations, such as the Taylor and Fourier series expansions, Bessel functions, trigonometric identities and the concept of the conduction angle, which simplify the circuit design procedure, are given.

1.1 SPECTRAL-DOMAIN ANALYSIS

The best way to understand the oscillator electrical behaviour and the fastest way to calculate its basic electrical characteristics such as output power, efficiency, phase noise, or harmonic suppression, is to use a spectral-domain analysis. Generally, such an analysis is based on the determination of the output response of the nonlinear active device when the multiharmonic

---

RF and Microwave Transistor Oscillator Design A. Grebennikov

signal is applied to its input port, which analytically can be written in the form

$$i(t) = f[v(t)] \tag{1.1}$$

where $i(t)$ is the output current, $v(t)$ is the input voltage and $f(v)$ is the nonlinear transfer function of the device. Unlike the spectral-domain analysis, time-domain analysis establishes the relationships between voltage and current in each circuit element in the time domain when a system of nonlinear integrodifferential equations is obtained applying Kirchhoff's law to the circuit to be analysed.

The voltage $v(t)$ in frequency domain generally represents the multiple frequency signal at the device input in the form

$$v(t) = V_0 + \sum_{k=1}^{N} V_k \cos(\omega_k t + \phi_k) \tag{1.2}$$

where V_0 is the constant voltage, V_k is the voltage amplitude and ϕ_k is the phase of the kth-order harmonic component ω_k, $k = 1, 2, \ldots, N$, and N is the number of harmonics.

The spectral domain analysis based on substituting Equation (1.2) in Equation (1.1) for a particular nonlinear transfer function of the active device determines an output spectrum as a sum of the fundamental-frequency and higher-order harmonic components, the amplitudes and phases of which will determine the output signal spectrum. Generally, this is a complicated procedure which requires a harmonic balance technique to numerically calculate an accurate nonlinear circuit response. However, the solution can be found analytically in a simple way when it is necessary to estimate only the basic performance of on oscillator in the form of the output power and efficiency. In this case, a technique based on a piecewise-linear approximation of the device transfer function can provide a clear insight into the basic oscillator behaviour and its operation modes. It can also serve as a good starting point for a final computer-aided design and optimization procedure.

The result of the spectral-domain analysis is shown as a summation of the harmonic components, the amplitudes and phases of which will determine the output signal spectrum. This problem can be solved analytically by using trigonometric identities, piecewise-linear approximation or Bessel functions.

1.1.1 Trigonometric identities

The use of trigonometric identities is very convenient when the transfer characteristic of the nonlinear element can be represented by the power series

$$i = a_0 + a_1 v + a_2 v^2 + \ldots + a_n v^n \tag{1.3}$$

If the effect of the input signal represents a single harmonic oscillation in the form

$$v = V \cos(\omega t + \phi) \tag{1.4}$$

then, by substituting Equation (1.4) into Equation (1.3), the power series can be written as

$$i = a_0 + a_1 V \cos(\omega t + \phi) + a_2 V^2 \cos^2(\omega t + \phi) + \ldots + a_n V^n \cos^n(\omega t + \phi) \tag{1.5}$$

To represent the right-hand side of Equation (1.5) as a sum of first-order cosine components, the following trigonometric identities, which replace the nth-order cosine components, can be used:

$$\cos^2\psi = \frac{1}{2}(1 + \cos 2\psi) \tag{1.6}$$

$$\cos^3\psi = \frac{1}{4}(3\cos\psi + \cos 3\psi) \tag{1.7}$$

$$\cos^4\psi = \frac{1}{8}(3 + 4\cos 2\psi + \cos 4\psi) \tag{1.8}$$

$$\cos^5\psi = \frac{1}{16}(10\cos\psi + 5\cos 3\psi + \cos 5\psi) \tag{1.9}$$

where $\psi = \omega t + \phi$.

By using the appropriate substitutions from Equations (1.6–1.9) and equating the signal frequency component terms, Equation (1.5) can be rewritten as

$$i = I_0 + I_1\cos(\omega t + \phi) + I_2\cos 2(\omega t + \phi) + I_3\cos 3(\omega t + \phi) + \ldots + I_n\cos n(\omega t + \phi) \tag{1.10}$$

where

$$I_0 = a_0 + \frac{1}{2}a_2V^2 + \frac{3}{8}a_4V^4 + \ldots$$

$$I_1 = a_1V + \frac{3}{4}a_3V^3 + \frac{5}{8}a_5V^5 + \ldots$$

$$I_2 = \frac{1}{2}a_2V^2 + \frac{1}{2}a_4V^4 + \ldots$$

$$I_3 = \frac{1}{4}a_3V^3 + \frac{5}{16}a_5V^5 + \ldots$$

Comparing Equations (1.3) and (1.10), we find:

- For nonlinear elements, the output spectrum contains frequency components which are multiples of the input signal frequency. The number of the highest-frequency component is equal to the maximum degree of the power series. Therefore, if it is necessary to know the amplitude of n-harmonic response, the volt–ampere characteristic of nonlinear element should be approximated by not less than an n-order power series.
- The output dc and even-order harmonic components are determined only by the even voltage degrees in the device transfer characteristic given by Equation (1.3). The odd-order harmonic components are defined only by the odd voltage degrees for the single harmonic input signal given by Equation (1.4).
- The current phase ψ_k of the kth-order harmonic component $\omega_k = k\omega$ is k times larger than the input signal current phase ψ:

$$\psi_k = \omega_k t + \phi_k = k(\omega t + \phi) \tag{1.11}$$

that is also applied to their initial phases defined as

$$\phi_k = k\phi \tag{1.12}$$

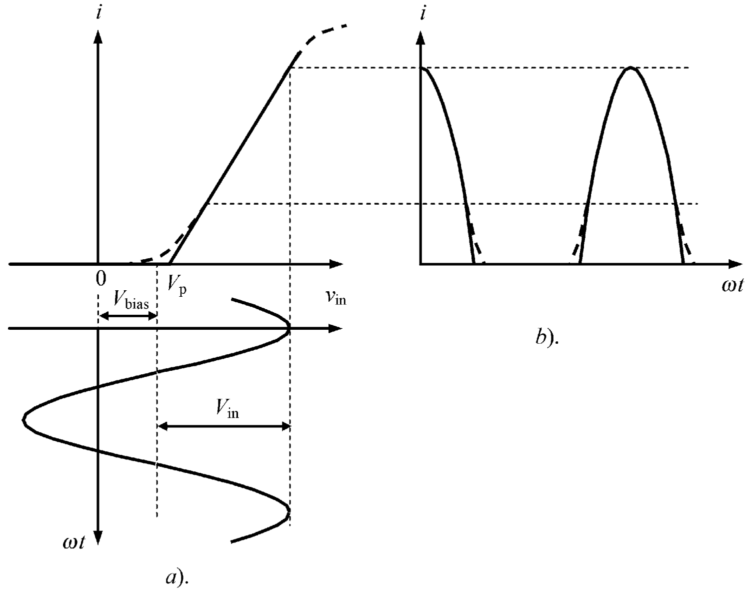

Figure 1.1 Piecewise-linear approximation technique

1.1.2 Piecewise-linear approximation

The piecewise-linear approximation of the active device current–voltage transfer characteristic is a result of replacing the actual nonlinear dependence $i = f(v_{in})$, where v_{in} the voltage applied to the device input, by an approximate one that consists of straight lines tangential to the actual dependence at the specified points. Such a piecewise-linear approximation for the case of two straight lines is shown in Figure 1.1a.

The output current waveforms for the actual current–voltage dependence (dashed curve) and its piecewise-linear approximation by two straight lines (solid curve) are plotted in Figure 1.1b. Under large-signal operation mode, the waveforms corresponding to these two dependencies are practically the same for the most part with negligible deviation for small values of the output current close to the pinch-off region of the device operation and significant deviation close to the saturation region of the device operation. However, the latter case results in a significant nonlinear distortion and is used only for high-efficiency operation modes when the active period of the device operation is minimized. Hence, at least two first output current components, dc and fundamental, can be calculated through a Fourier series expansion with a sufficient accuracy. Therefore, such a piecewise-linear approximation with two straight lines can be effective for a quick estimate of the oscillator output power and efficiency.

In this case, the piecewise-linear active device transfer current–voltage characteristic is defined by

$$i = \begin{cases} 0 & v_{in} \le V_p \\ g_m(v_{in} - V_p) & v_{in} \ge V_p \end{cases} \tag{1.13}$$

where g_m is the device transconductance, V_p is the pinch-off voltage.

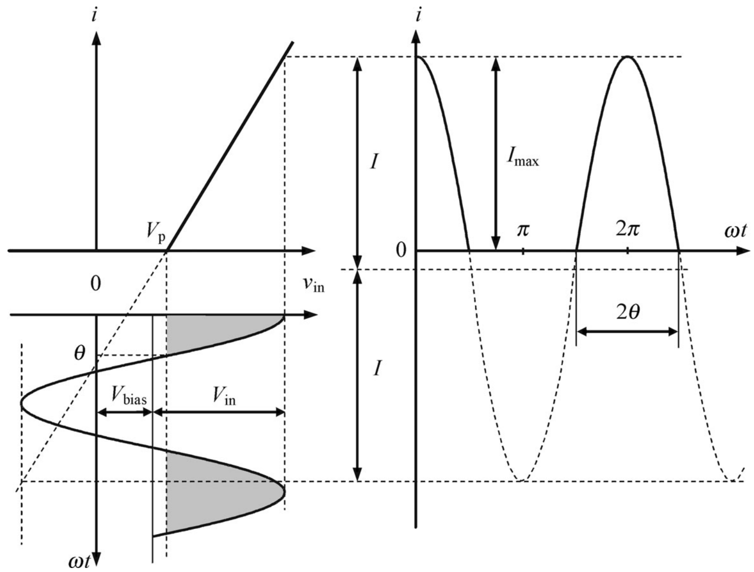

Figure 1.2 Schematic definition of conduction angle

Let us assume the input signal to be of cosinusoidal form

$$v_{in} = V_{bias} + V_{in} \cos \omega t \tag{1.14}$$

where V_{bias} is the input dc bias voltage.

At the point on the plot when voltage $v_{in}(\omega t)$ becomes equal to a pinch-off voltage V_p and where $\omega t = \theta$, the output current $i(\theta)$ has value zero. At this moment

$$V_p = V_{bias} + V_{in} \cos \theta \tag{1.15}$$

and θ can be calculated from

$$\cos \theta = -\frac{V_{bias} - V_p}{V_{in}} \tag{1.16}$$

As a result, the output current represents a periodic pulsed waveform described by the cosinusoidal pulses with the maximum amplitude I_{max} and width 2θ as

$$i = \begin{cases} I_q + I \cos \omega t & -\theta \le \omega t < \theta \\ 0 & \theta \le \omega t < 2\pi - \theta \end{cases} \tag{1.17}$$

where the conduction angle 2θ indicates the part of the RF current cycle during which device conduction occurs, as shown in Figure 1.2. When the output current $i(\omega t)$ has value zero, one can write

$$i = I_q + I \cos \theta = 0 \tag{1.18}$$

Taking into account that, for a piecewise-linear approximation, $I = g_m V_{in}$, Equation (1.17) can be rewritten as

$$i = g_m V_{in}(\cos \omega t - \cos \theta) \tag{1.19}$$

When $\omega t = 0$, then $i = I_{\max}$ and

$$I_{\max} = I(1 - \cos\theta) \tag{1.20}$$

The angle θ characterizes the class of the active device operation. If $\theta = \pi$ or 180°, the device operates in the active region during the entire period (class A operation). When $\theta = \pi/2$ or 90°, the device operates half a wave period in the active region and half a wave period in the pinch-off region (class B operation). The values of $\theta > 90°$ correspond to class AB operation with a certain value of the quiescent output current. Therefore, the double angle 2θ is called the conduction angle, the value of which directly indicates the class of the active device operation.

The Fourier series expansion of the even function when $i(t) = i(-t)$ contains only even component functions and can be written as

$$i(t) = I_0 + I_1 \cos\omega t + I_2 \cos 2\omega t + I_3 \cos 3\omega t + \ldots \tag{1.21}$$

where the dc, fundamental-frequency and nth-order harmonic components are calculated by

$$I_0 = \frac{1}{2\pi} \int_{-\theta}^{\theta} g_{\mathrm{m}} V_{\mathrm{in}} (\cos\omega t - \cos\theta)\, d(\omega t) = \gamma_0(\theta) I \tag{1.22}$$

$$I_1 = \frac{1}{\pi} \int_{-\theta}^{\theta} g_{\mathrm{m}} V_{\mathrm{in}} (\cos\omega t - \cos\theta) \cos\omega t \, d(\omega t) = \gamma_1(\theta) I \tag{1.23}$$

$$I_{\mathrm{n}} = \frac{1}{\pi} \int_{-\theta}^{\theta} g_{\mathrm{m}} V_{\mathrm{in}} (\cos\omega t - \cos\theta) \cos(n\omega t)\, d(\omega t) = \gamma_{\mathrm{n}}(\theta) I \tag{1.24}$$

where $\gamma_n(\theta)$ are called the coefficients of expansion of the output current cosinusoidal pulse or the current coefficients [1]. They can be analytically defined as

$$\gamma_0(\theta) = \frac{1}{\pi}(\sin\theta - \theta\cos\theta) \tag{1.25}$$

$$\gamma_1(\theta) = \frac{1}{\pi}\left(\theta - \frac{\sin 2\theta}{2}\right) \tag{1.26}$$

$$\gamma_n(\theta) = \frac{1}{\pi}\left[\frac{\sin(n-1)\theta}{n(n-1)} - \frac{\sin(n+1)\theta}{n(n+1)}\right] \tag{1.27}$$

where $n = 2, 3, \ldots$.

The dependencies of $\gamma_n(\theta)$ for the dc, fundamental-frequency, second- and higher-order current components are shown in Figure 1.3. The maximum value of $\gamma_n(\theta)$ is achieved when $\theta = 180°/n$. A special case is $\theta = 90°$, when odd current coefficients are equal to zero, i.e., $\gamma_3(\theta) = \gamma_5(\theta) = \ldots = 0$. The ratio between the fundamental-frequency and dc components $\gamma_1(\theta)/\gamma_0(\theta)$ varies from 1 to 2 for any values of the conduction angle, with a minimum value of 1 for $\theta = 180°$ and a maximum value of 2 for $\theta = 0°$. It is necessary to pay attention to the fact that, for example, the current coefficient $\gamma_3(\theta)$ becomes negative within the interval of $90° < \theta < 180°$. This implies appropriate phase changes of the third current harmonic component when its values are negative. Consequently, if the harmonic components for which

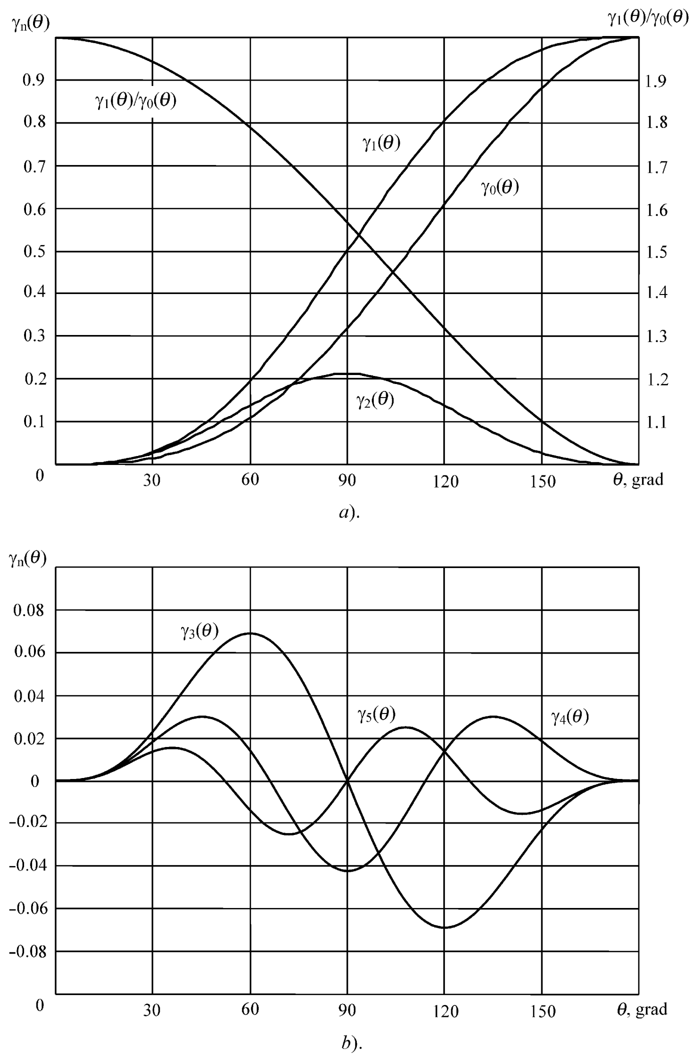

Figure 1.3 Dependencies of $\gamma_n(\theta)$ for dc, fundamental- and higher-order current components

$\gamma_n(\theta) > 0$ achieve positive maximum values at times corresponding to the midpoints of the current waveform, the harmonic components for which $\gamma_n(\theta) < 0$ can achieve negative maximum values at these times. As a result, combination of different harmonic components with proper loading will result in flattening of the current or voltage waveforms, thus improving efficiency of the oscillator. The amplitude of corresponding current harmonic component can be obtained as

$$I_n = \gamma_n(\theta) g_m V_{in} = \gamma_n(\theta) I \tag{1.28}$$

Sometimes it is necessary for an active device to provide a constant value of I_{max} at any value of θ. This requires an appropriate variation of the input voltage amplitude V_{in}. In this case, it is more convenient to use the other coefficients when the nth-order current harmonic amplitude I_n is related to the maximum current waveform amplitude $I_{\max}$, that is

$$\alpha_n = \frac{I_n}{I_{\max}} \tag{1.29}$$

From Equations (1.20), (1.28) and (1.29) it follows that

$$\alpha_n = \frac{\gamma_n(\theta)}{1 - \cos\theta} \tag{1.30}$$

and the maximum value of $\alpha_n(\theta)$ is achieved when $\theta = 120^\circ/n$.

1.1.3 Bessel functions

The Bessel functions are used to analyse the oscillator operation mode when a nonlinear behaviour of the active device can be described by exponential functions. The transfer voltage–ampere characteristic of the bipolar transistor is approximated by the simplified exponential dependence neglecting reverse base–emitter current as

$$i(v_{\text{in}}) = I_{\text{sat}}\left[\exp\left(\frac{v_{\text{in}}}{V_T}\right) - 1\right] \tag{1.31}$$

where I_{sat} is the minority carrier saturation current and V_T is the temperature voltage. If the effect of the input signal given by Equation (1.14) is considered, then Equation (1.31) can be rewritten as

$$i(\omega t) = I_{\text{sat}}\left[\exp\left(\frac{V_{\text{bias}}}{V_T}\right)\exp\left(\frac{V_{\text{in}}\cos\omega t}{V_T}\right) - 1\right] \tag{1.32}$$

The current $i(\omega t)$ in Equation (1.32) is the even function of ωt and, consequently, it can be represented by the Fourier-series expansion given by Equation (1.21). To determine the Fourier components, the following expression is used:

$$\exp\left(\frac{V_{\text{in}}\cos\omega t}{V_T}\right) = I_0\left(\frac{V_{\text{in}}}{V_T}\right) + 2\sum_{k=1}^{\infty} I_k\left(\frac{V_{\text{in}}}{V_T}\right)\cos(k\omega t) \tag{1.33}$$

where $I_k(V_{\text{in}}/V_T)$ are the kth-order modified Bessel functions of the first kind for an argument of V_{in}/V_T, shown in Figure 1.4 for the zeroth- and first-order components. It should be noted that $I_0(0) = 1$ and $I_1(0) = I_2(0) = \ldots = 0$, and with an increase of the component number its amplitude appropriately decreases.

According to Equation (1.33), the current $i(\omega t)$ defined by Equation (1.31) can be rewritten as

$$\begin{aligned} i(\omega t) = I_{\text{sat}}&\left[\exp\left(\frac{V_{\text{bias}}}{V_T}\right) I_0\left(\frac{V_{\text{in}}}{V_T}\right) - 1\right] + 2I_{\text{sat}}\exp\left(\frac{V_{\text{bias}}}{V_T}\right) I_1\left(\frac{V_{\text{in}}}{V_T}\right)\cos(\omega t) \\ &+ 2I_{\text{sat}}\exp\left(\frac{V_{\text{bias}}}{V_T}\right) I_2\left(\frac{V_{\text{in}}}{V_T}\right)\cos(2\omega t) + 2I_{\text{sat}}\exp\left(\frac{V_{\text{bias}}}{V_T}\right) I_3\left(\frac{V_{\text{in}}}{V_T}\right)\cos(3\omega t) + \ldots \end{aligned} \tag{1.34}$$

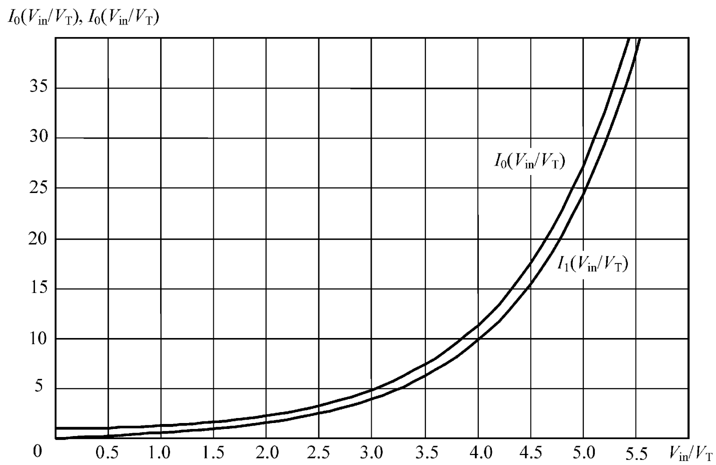

Figure 1.4 Zeroth- and first-order modified Bessel functions of the first kind

As a result, comparing Equations (1.34) and (1.21) allows the dc, fundamental-frequency and nth-order Fourier current components to be determined as

$$I_0 = I_{sat}\left[\exp\left(\frac{V_{bias}}{V_T}\right) I_0\left(\frac{V_{in}}{V_T}\right) - 1\right] \tag{1.35}$$

$$I_1 = 2I_{sat}\exp\left(\frac{V_{bias}}{V_T}\right) I_1\left(\frac{V_{in}}{V_T}\right) \tag{1.36}$$

$$I_n = 2I_{sat}\exp\left(\frac{V_{bias}}{V_T}\right) I_n\left(\frac{V_{in}}{V_T}\right) \tag{1.37}$$

where $n = 2, 3, \ldots$.

When using the Bessel functions, the following relationships can be helpful:

$$2\frac{\mathrm{d}I_n\left(V_{in}/V_T\right)}{\mathrm{d}\left(V_{in}/V_T\right)} = I_{n+1}\left(\frac{V_{in}}{V_T}\right) + I_{n-1}\left(\frac{V_{in}}{V_T}\right) \tag{1.38}$$

$$\frac{\mathrm{d}I_0\left(V_{in}/V_T\right)}{\mathrm{d}\left(V_{in}/V_T\right)} = I_1\left(\frac{V_{in}}{V_T}\right) \tag{1.39}$$

$$\frac{2n}{\left(V_{in}/V_T\right)} I_n\left(\frac{V_{in}}{V_T}\right) = I_{n-1}\left(\frac{V_{in}}{V_T}\right) - I_{n+1}\left(\frac{V_{in}}{V_T}\right) \tag{1.40}$$

$$I_n\left(-\frac{V_{in}}{V_T}\right) = (-1)^n I_n\left(\frac{V_{in}}{V_T}\right) \tag{1.41}$$

1.2 TIME-DOMAIN ANALYSIS

A time-domain analysis establishes the relationships between voltage and current in each circuit element in the time domain when a system of equations is obtained, applying Kirchhoff's law to the circuit to be analysed. Normally, in a nonlinear circuit, such a system will be composed of nonlinear integrodifferential equations. The solution to this system can be found by applying numerical integration methods. Therefore, the choices of the time interval and the initial point are very important to provide a compromise between speed and accuracy of calculation; the smaller the interval, the smaller the error, but the number of points to be calculated for each period will be greater, which will make the calculation slower.

To analyse a nonlinear system in the time domain, it is necessary to know the voltage–current relationships for all circuit elements. For example, for linear resistance R, when the sinusoidal voltage applies and current are flowing through it, the voltage–current relationship in the time domain is given by

$$V = RI \tag{1.42}$$

where V is the voltage amplitude and I is the current amplitude.

For linear capacitance C

$$i(t) = \frac{\mathrm{d}q(t)}{\mathrm{d}t} = \frac{\mathrm{d}q}{\mathrm{d}v}\frac{\mathrm{d}v}{\mathrm{d}t} = C\frac{\mathrm{d}v}{\mathrm{d}t} \tag{1.43}$$

For linear inductance L

$$v(t) = \frac{\mathrm{d}\varphi(t)}{\mathrm{d}t} = \frac{\mathrm{d}\varphi}{\mathrm{d}i}\frac{\mathrm{d}i}{\mathrm{d}t} = L\frac{\mathrm{d}i}{\mathrm{d}t} \tag{1.44}$$

where φ is the magnetic flux across the inductance.

Nonlinear dependencies, such as $q(v)$ or $\varphi(i)$, should each be expanded in a Taylor series by subtracting the dc components and substituting into Equations (1.43) and (1.44) to obtain the expressions for appropriate incremental capacitance and inductance. Then, for the quasilinear case, the capacitance and inductance can be defined by

$$C(V_0) = \left.\frac{\mathrm{d}q(v)}{\mathrm{d}v}\right|_{v=V_0} \tag{1.45}$$

and

$$L(I_0) = \left.\frac{\mathrm{d}\varphi(i)}{\mathrm{d}i}\right|_{i=I_0} \tag{1.46}$$

where V_0 is the dc bias voltage across the capacitor and I_0 is the dc current flowing through the inductor.

Figure 1.5 shows the simplified (without bias circuits) electrical schematic of a transformer-coupled MOSFET oscillator with a parallel resonant circuit. To obtain the differential equations

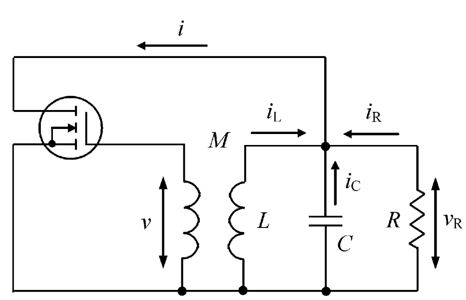

Figure 1.5 Schematic of a transformer-coupled MOSFET oscillator

for such an oscillator, the drain current i, the gate voltage v applied to the second winding of the transformer, and the load voltage v_R applied to the first winding of this transformer can be defined by

$$i = i_L + i_C + i_R \tag{1.47}$$

$$v_R = L\frac{di_L}{dt} = \frac{1}{C}\int i_C dt = i_R R \tag{1.48}$$

$$v = M\frac{di_L}{dt} = \frac{M}{L}v_R \tag{1.49}$$

where M is the transformer coupling factor.

To simplify the calculation, two preliminary assumptions can be used:

- the input current flowing to the gate terminal of the active device is negligible, enabling one to consider its input impedance as infinite;
- the effect of the output voltage v_R on the drain current i is ignored, i.e.,

$$i = f(v). \tag{1.50}$$

In this case, the derivative of current $i(v)$ with respect to time is written as

$$\frac{di}{dt} = \frac{di}{dv}\frac{dv}{dt} = g_m(v)\frac{dv}{dt} \tag{1.51}$$

where $g_m = di/dv$ is the small-signal transconductance of the device transfer characteristic given by Equation (1.50).

Substituting Equations (1.48) and (1.50) into Equation (1.47) gives

$$\frac{1}{L}\int v_R dt + C\frac{dv_R}{dt} + \frac{v_R}{R} = f(v) \tag{1.52}$$

Then, by differentiating Equation (1.52) and using Equations (1.49) and (1.51), we can write the second-order differential equation for the oscillator in the form

$$\frac{d^2v}{dt^2} + \frac{1}{C}\left[\frac{1}{R} - \frac{Mg_m(v)}{L}\right]\frac{dv}{dt} + \omega_0^2 v = 0 \tag{1.53}$$

where

$$\omega_0 = \frac{1}{\sqrt{LC}}$$

is the oscillator resonant frequency.

Equation (1.53) is a nonlinear equation because its second term depends on the unknown variable v. This nonlinearity is a result of the active device nonlinearity. From Equation (1.53), the start-up and steady-state oscillation conditions can be determined, as well as the particular features of the steady-state oscillations and oscillator transient response. To determine the start-up conditions, it is necessary to replace nonlinear Equation (1.53) by an appropriate linear one, with the linear small-signal transconductance g_m at the operating bias point. In this case, we are interested only in the result of the small deviation from an equilibrium point, whether the oscillations will grow or dissipate.

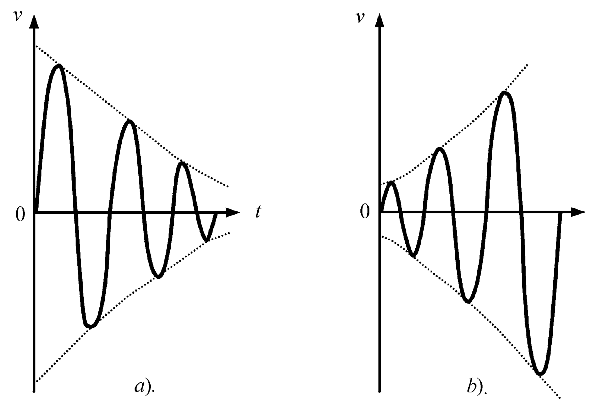

Figure 1.6 Oscillations with (a) low and (b) strong feedback factors

The solution of such a linear second-order differential equation is

$$v = V \exp(-\delta t) \sin(\omega_1 t + \phi) \tag{1.54}$$

where V and ϕ are the voltage amplitude and phase, respectively, depending on the initial conditions,

$$\delta = \frac{1}{2C}\left(\frac{1}{R} - \frac{M g_{\mathrm{m}}}{L}\right) \tag{1.55}$$

is the dissipation factor, and

$$\omega_1 = \sqrt{\omega_0^2 - \delta^2} \tag{1.56}$$

is the free-running oscillation frequency.

From Equation (1.54) it follows that the voltage v at the device input provided by the feedback circuit creates current i at the device output, which delivers electrical energy to the oscillation system to compensate for the losses in it. At the same time, the required value of this energy is the result of the transformation of the energy of the dc current delivered from the dc current source to the energy of the ac current. If the feedback factor is sufficiently small when $\delta > 0$, the delivered energy compensates for the dissipated energy only partly. As a result, this leads to attenuation and dissipation of the oscillations, as shown in Figure 1.6a. For strong feedback factor when $\delta < 0$, the delivered energy exceeds the dissipated energy, and the oscillations increase with time, as shown in Figure 1.6b.

1.3 NEWTON–RAPHSON ALGORITHM

To describe circuit behaviour, it is necessary to solve the nonlinear algebraic equation, or system of equations, which do not generally admit a closed form solution analytically. One of the most common numerical methods to solve such equations is a method based on the Newton–Raphson algorithm [2]. The initial guess for this method is chosen using a Taylor series expansion of the nonlinear function. Consider a practical case when the device is represented by a two-port network where all nonlinear elements are functions of the two unknown voltages, input voltage

v_{in} and output voltage v_{out}. As a result, after combining linear and nonlinear circuit elements, a system of two equations can be written as

$$f_1(v_{\text{in}}, v_{\text{out}}) = 0 \tag{1.57}$$

$$f_2(v_{\text{in}}, v_{\text{out}}) = 0 \tag{1.58}$$

Assume that the variables v_{in0} and v_{out0} are the initial approximate solution of a system of Equations (1.57) and (1.58). Then, the variables can be written as $v_{\text{in}} = v_{\text{in0}} + \Delta v_{\text{in}}$ and $v_{\text{out}} = v_{\text{out0}} + \Delta v_{\text{out}}$, where Δv_{in} and Δv_{out} are the linear increments of the variables. Applying a Taylor series expansion to Equations (1.57) and (1.58) yields

$$f_1(v_{\text{in0}} + \Delta v_{\text{in}}, v_{\text{out0}} + \Delta v_{\text{out}}) = f_1(v_{\text{in0}}, v_{\text{out0}}) + \left.\frac{\partial f_1}{\partial v_{\text{in}}}\right|_{\substack{v_{\text{in}}=v_{\text{in0}}\\ v_{\text{out}}=v_{\text{out0}}}} \Delta v_{\text{in}}$$
$$+ \left.\frac{\partial f_1}{\partial v_{\text{out}}}\right|_{\substack{v_{\text{in}}=v_{\text{in0}}\\ v_{\text{out}}=v_{\text{out0}}}} \Delta v_{\text{out}} + o\left(\Delta v_{\text{in}}^2 + \Delta v_{\text{out}}^2 + \ldots\right) = 0 \tag{1.59}$$

$$f_2\,(v_{\text{in0}} + \Delta v_{\text{in}}, v_{\text{out0}} + \Delta v_{\text{out}}) = f_2\,(v_{\text{in0}}, v_{\text{out0}}) + \left.\frac{\partial f_2}{\partial v_{\text{in}}}\right|_{\substack{v_{\text{in}}=v_{\text{in0}}\\ v_{\text{out}}=v_{\text{out0}}}} \Delta v_{\text{in}}$$
$$+ \left.\frac{\partial f_2}{\partial v_{\text{out}}}\right|_{\substack{v_{\text{in}}=v_{\text{in0}}\\ v_{\text{out}}=v_{\text{out0}}}} \Delta v_{\text{out}} + o\left(\Delta v_{\text{in}}^2 + \Delta v_{\text{out}}^2 + \ldots\right) = 0 \tag{1.60}$$

where $o(\Delta v_{\text{in}}^2 + \Delta v_{\text{out}}^2 + \ldots)$ denotes the second- and higher-order components.

By neglecting the second- and higher-order components, Equations (1.59) and (1.60) can be rewritten in matrix form

$$-\begin{bmatrix} f_1 \\ f_2 \end{bmatrix} = \begin{bmatrix} \dfrac{\partial f_1}{\partial v_{\text{in}}} & \dfrac{\partial f_1}{\partial v_{\text{out}}} \\ \dfrac{\partial f_2}{\partial v_{\text{in}}} & \dfrac{\partial f_2}{\partial v_{\text{out}}} \end{bmatrix} \begin{bmatrix} \Delta v_{\text{in}} \\ \Delta v_{\text{out}} \end{bmatrix} \tag{1.61}$$

In the phasor form,

$$-\boldsymbol{F} = \boldsymbol{J}\Delta\boldsymbol{v} \tag{1.62}$$

where $\boldsymbol{J}$ is the Jacobian matrix of a system of Equations (1.57) and (1.58).

The solution of Equation (1.62) for a nonsingular matrix $\boldsymbol{J}$ can be obtained by

$$\Delta\boldsymbol{v} = -\boldsymbol{J}^{-1}\boldsymbol{F} \tag{1.63}$$

This means that if

$$\boldsymbol{v}_0 = \begin{bmatrix} v_{\text{in0}} \\ v_{\text{out0}} \end{bmatrix} \tag{1.64}$$

is the initial guess of this system of equation, then the next (more precise) solution can be written as

$$\boldsymbol{v}_1 = \boldsymbol{v}_0 - \boldsymbol{J}^{-1}\boldsymbol{F} \tag{1.65}$$

where

$$\boldsymbol{v}_1 = \begin{bmatrix} v_{\text{in1}} \\ v_{\text{out1}} \end{bmatrix} \tag{1.66}$$

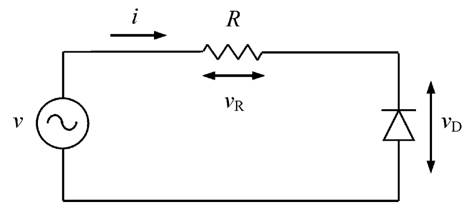

Figure 1.7 Circuit schematic with resistor, diode, and voltage source

Thus, starting with initial guess $\boldsymbol{v}_0$, we compute $\boldsymbol{v}_1$ at the first iteration. For the iteration $n+1$, we can write

$$\boldsymbol{v}_{n+1} = \boldsymbol{v}_n - \boldsymbol{J}^{-1}\boldsymbol{F}(\boldsymbol{v}_n) \tag{1.67}$$

The iterative Equation (1.67) is given for a system of two equations; however it can be directly extended to a system of k nonlinear equations with k unknown parameters. This iterative procedure is terminated after $(n+1)$ iterations whenever

$$|\boldsymbol{x}_{n+1} - \boldsymbol{x}_n| = \sqrt{\sum_{k=1}^{K}\left(x_{n+1}^k - x_n^k\right)^2} < \varepsilon \tag{1.68}$$

where ε is a small positive number depending on the desired accuracy. For a practical purpose, it is desirable that the Newton–Raphson algorithm should converge in a few steps. Therefore, the choice of an appropriate initial guess is crucial to the success of the algorithm.

Consider the circuit shown in Figure 1.7. According to Kirchhoff's voltage law,

$$v = v_{\mathrm{R}} + v_{\mathrm{D}} \tag{1.69}$$

where $v_{\mathrm{R}} = iR$.

The electrical behaviour of the diode is described by

$$i(v_{\mathrm{D}}) = I_{\mathrm{sat}}\left[\exp\left(\frac{v_{\mathrm{D}}}{V_T}\right) - 1\right] \tag{1.70}$$

Rearranging Equation (1.70) gives the equation for v_{D} in the form

$$v_{\mathrm{D}} = V_T \ln\left(\frac{i}{I_{\mathrm{sat}}} + 1\right) \tag{1.71}$$

Thus, from Equations (1.60) and (1.61) it follows that

$$v = iR + V_T \ln\left(\frac{i}{I_{\mathrm{sat}}} + 1\right) \tag{1.72}$$

This allows current i to be determined for a specified voltage v. However, because it is impossible to solve this equation analytically for current i in explicit form, the solution must be found numerically.

Consider a dc voltage source V with dc current I. For the sinusoidal voltage source, it is necessary to calculate the Bessel functions for dc, fundamental-frequency and higher-order